16L2: OPERATION, OBSERVATIONS AND PHYSICS ASPECTS

L. Mether*, EPFL, Lausanne, Switzerland
D. Amorim, G. Arduini, X. Buffat, G. Iadarola, A. Lechner, E. Métral,
D. Mirarchi, G. Rumolo, B. Salvant, CERN, Geneva, Switzerland

Abstract

Events linked to fast losses in the LHC half-cell 16L2 have plagued a large part of the 2017 run. While a detailed analysis of what happened is treated at the LHC Performance Workshop (Chamonix 2018), this contribution will gather the available observations and the understanding of the situation as predicted by simulations and models, before the warm-up during the 2017 year-end technical stop (YETS). The impact of the 16L2 events on the global LHC performance in 2017 will also be evaluated.

INTRODUCTION

Since the start of 2017 operation, abnormal losses were observed by the beam loss monitors in the LHC half-cell 16L2 (see Fig. 1) [1]. During the year, in total 68 premature dumps linked to losses in 16L2 occurred (see Fig. 2). The events could be characterised by the following signature: a sudden onset of high beam losses in 16L2, coherent beam motion with very fast rise times, and eventually a beam dump due to losses either on the collimation system, or directly in the half-cell 16L2. In order to stay operational, the LHC was limited to around 25% fewer than the nominal number of bunches for most of the 2017 run, as is illustrated in Fig. 2.

From an early stage, several observations pointed to the issue being related to a local vacuum degradation. Firstly, the losses, which occurred on both beams in the same location, indicated the presence of nuclei in the beam vacuum. Furthermore, the losses occurred in a location where a pumping module was connected to both magnet apertures during the 2016–2017 extended year-end technical stop (EYETS), when Sector 12 was opened for the exchange of a faulty dipole magnet. In addition, unexpectedly high pressures were observed by additional vacuum gauges installed in 16L2 during the beam screen regeneration (marked in Fig. 2), which consists of increasing the beam screen temperature to approximately 80 K, although the issue was not resolved [2]. These observations led to the suspicion that some air could have been let in around 16L2 during the cool-down of Sector 12, and condensed on the cold surfaces as a frost, consisting mainly of nitrogen and oxygen. The hypothesis was confirmed during the complete beam screen and cold-bore warm-up to 80 K that took place after the end of the 2017 run, where observations were consistent with several litres of air having entered each beam line in 16L2 [3].

LOSS OBSERVATIONS AND MODELLING

The losses observed in 16L2 provided one of the most important pieces of information for the understanding of the sequence of events leading to the beam dumps. Since the losses are produced by inelastic collisions of beam particles with nuclei, the observed longitudinal pattern in the beam loss monitors (BLMs) allows estimating the location of the nuclei based on energy deposition simulations. With the aid of additional mobile BLMs that were installed in 16L2 for improved diagnostics, the location of the losses could be determined to within roughly 1.3 meters, to the region of the MCB.16L2 dipole corrector and/or the interconnection between the 16L2 quadrupole and its neighbouring dipole [4]. The measured beam loss pattern during a 16L2 event and the simulated loss pattern are shown in Fig. 1. The loss patterns were very similar for all the dump events, and there was no significant change observed in the loss location after the beam screen regeneration.

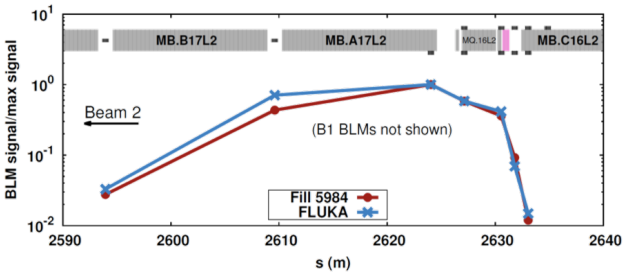

Figure 1: Measured and simulated BLM patterns for a beam loss event in 16L2 at 6.5 TeV [4].

During the operational year, three distinct types of losses could be observed in 16L2 [5]:

- **Steady-state losses**
  Loss rates up to a few μGy/s (around a factor 10 higher than the background) were observed throughout fills from the beginning of operation [6]. Such losses were significantly reduced by the beam screen regeneration.

- **UFO-like spikes**
  Loss spikes of millisecond duration with loss rates up to several tens of mGy/s were observed sporadically. Such events on their own were not associated with coherent beam motion, nor with beam dumps, and were similar to standard dust particle, or UFO, events [7, 8].

- **Dump events**
  These events are characterised by an increasing rate of losses up to about a hundred mGy/s, over a duration from a few milliseconds to several tens of milliseconds. They were correlated with coherent motion and always ended with a beam dump. As shown in Fig. 3, such losses were often preceded by a UFO-like spike, as described above.

* lotta.mether@cern.ch

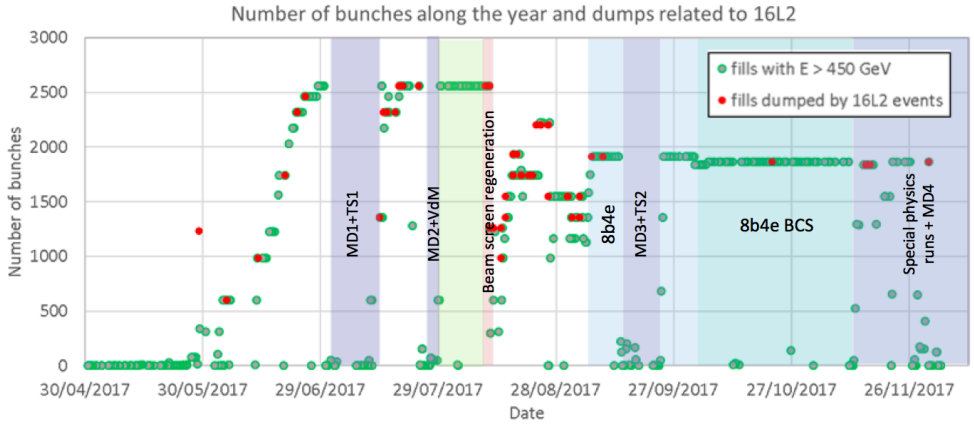

Figure 2: Overview of fills in 2017. The green markers show the number of bunches per beam for fills that reached an energy above the injection energy, while the red dots mark fills that were dumped due to events in 16L2.

All three types of losses were observed intermittently on each beam, and the loss pattern showed that the location of their source was very similar [9]. These considerations, together with the similarities between the UFO spikes and the initial stage of the dump events, point to a common origin for all three types of losses.

Assuming the presence of condensed air (nitrogen and/or oxygen) in the beam chamber, the different losses could be explained as follows. The steady-state losses may arise due to beam-gas scattering with out-gassed nitrogen or oxygen. The UFO-like spike events could be explained by a solid nitrogen/oxygen macro-particle that is detached from the condensate and intercepts the beam [7, 8]. As for typical UFO events involving dust particles, the macro-particle is heated and positively charged through Coulomb interactions with beam particles, and is eventually repelled by the beam. The dump events, on the other hand, although often initiated by a UFO-like spike, cannot be explained simply by a solid macro-particle entering the beam. Instead, such a loss pattern could arise if a macro-particle that enters the beam, as described above, is sufficiently heated up to undergo a phase transition to a gas [7, 10]. The subsequent presence of the gas, could explain both the continued high loss rate and the observed coherent effects. The loss pattern of a typical dump event is shown in Fig. 3, with the presumed transition from a solid macro-particle to the gas phase indicated.

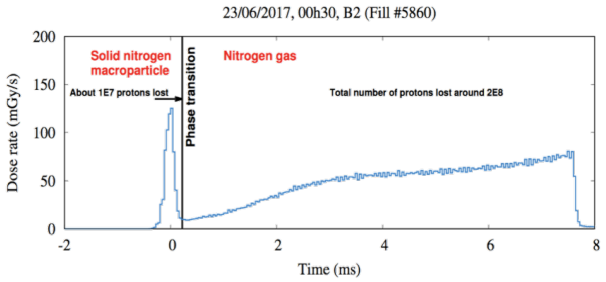

Figure 3: Measured loss rate as a function of time during a 16L2 dump event.

The possibility of a phase transition from solid to gas to occur for a nitrogen macro-particle has been studied based on loss observations and energy deposition studies [11]. The minimum required energy density for a transition from solid to gas can be estimated based on the phase diagram and specific heat of nitrogen to be around 110 J/g. Assuming a spherical macro-particle of radius r, the energy density deposited in it by the beam can be estimated to

$$\epsilon_d(N_i, r) = \left.\frac{dE}{dx}\right|_r N_i \lambda \frac{3}{4\pi r^3} , \qquad (1)$$

where $\left.\frac{dE}{dx}\right|_r$ is the restricted stopping power of beam protons in the macro-particle, N_i is the number of inelastic collisions of beam protons with nuclei in the macro-particle and λ is the inelastic scattering length for the macro-particle. The stopping power and scattering length can be determined by energy deposition simulations, whereas the number of inelastic collisions can be estimated from BLM signals.

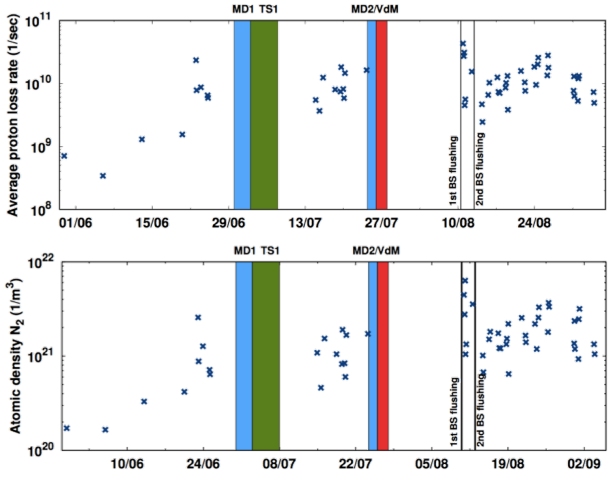

Figure 4: Measured loss rates (top) and estimated atomic densities (bottom) during beam loss events in 16L2 in 2017.

For a typical dump event, with an estimated 10^7 inelastic collisions during the loss peak, the energy density could become high enough (>110 J/g) to induce the phase transition to gas of a macro-particle with a radius around a few tens of micrometers. The macro-particle could thus lead to a local pressure bump, with significantly higher gas densities than expected for the residual gas. The atomic density during individual dump events can be estimated based on the measured loss rates [11]. Assuming that only nitrogen gas is present and that the pressure bump extends longitudinally over a distance of 10 cm and transversally over the full beam cross section, the atomic densities during the events in 2017 are estimated to lie in the range 10^{20} – 10^{22} m^{-3}, as illustrated in Fig. 4.

OBSERVATIONS AND MODELLING OF COHERENT EFFECTS

The 16L2 dump events were often associated with coherent beam motion. Several distinct patterns of unstable bunches were observed during different dump events [12]. In some events, only a few bunches at the head of the bunch trains were oscillating, while in others coupled-bunch motion over a large part of the bunches could be observed. In some cases the first pattern could be seen initially, followed later by the second one. In other events, only a small-amplitude oscillation over the full beam could be detected. When significant coherent oscillations occurred, the unstable motion developed very fast, typically with rise times shorter than 100 turns [13]. This is faster than expected from known instability driving mechanisms for the LHC at 6.5 TeV, such as impedance or electron cloud. Attempts to mitigate the instability with standard techniques, e.g. by increasing the Landau damping with octupole magnets or increasing the damping rate of the transverse feedback, were unsuccessful, as anticipated for such fast instabilities.

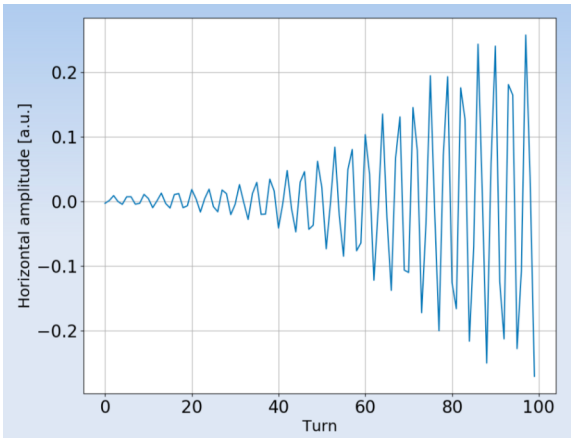

Figure 5: Coherent motion observed during a 16L2 event.

Due to the very fast development of the dump events, it was rarely possible to acquire sufficient data for further analysis of the unstable motion. In a few events, however, the headtail monitor, which was set up to record the last 11 turns of dump events, detected a clear signal of intra-bunch motion [14]. In these cases, intra-bunch motion affecting in particular the tail of the bunches was observed, as shown in Fig. 6a. Furthermore, during slower events, where the instabilities evolved for a sufficient number of turns before the beam dump, it was also possible to perform frequency analysis of the unstable motion to deduce the single bunch coherent tunes [15]. In these cases, positive tune shifts of magnitudes up to 2×10^{-2} were observed. An example of measured tune shifts during a 16L2 event is shown in Fig. 6b.

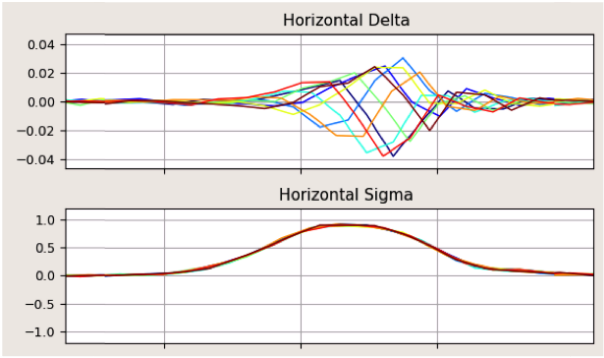

(a) Intra-bunch motion during the last turns of a 16L2 event. The head of the bunch is on the left and the tail on the right.

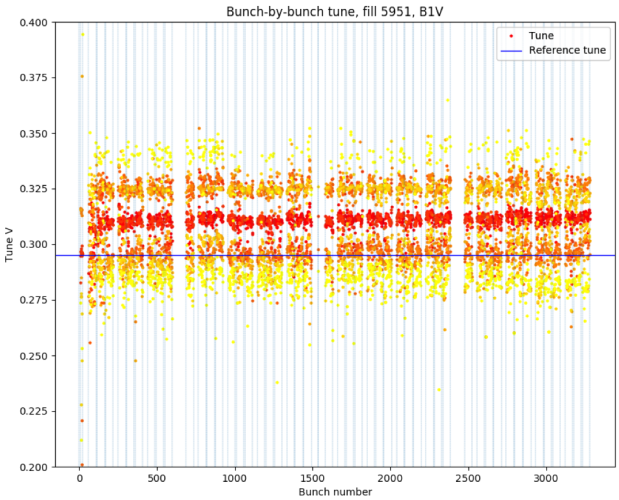

(b) Bunch-by-bunch coherent tunes during a 16L2 event. The reference tune is indicated by the blue line.

Figure 6: Measurements during 16L2 events.

Since the instabilities were much faster than expected from impedance or electron cloud, it was initially speculated whether they could be caused by ions [16]. However, both the observed intra-bunch motion and the tune shifts suggest that electrons likely play an important role in the instability mechanism. Intra-bunch motion concentrated at the tail of bunches is a typical signature of fast electron cloud instabilities [17], whereas ions are too slow to move significantly on the time scale of a bunch passing, and therefore are not expected to cause significant intra-bunch motion. In addition, a positive tune shift can be caused by a concentration

of negative charge in the core of the beam [18]. In order to induce the observed fast rise times and the large positive tune shifts, however, the electron densities involved must be significantly higher than expected in standard electron clouds in the machine.

The required electron density for a tune shift of 10^{-2} could be estimated based on analytical models to around 5×10^{17} m^{-3} if stretched over a 10 cm length [19]. An equivalent broad-band resonator impedance model for an electron cloud could also roughly reproduce the observed rise time and intra-bunch motion, with a shunt impedance $R_s = 150 - 500$ MΩ/m at the frequency $f_r = 2.6$ GHz [20]. Macro-particle simulations of the beam-electron interaction confirm that an electron density of 10^{17} m^{-3} over 10 cm may lead to similar rise times, tune shifts and intra-bunch motion as observed [21]. However, simulations also show that such a large electron density on its own cannot easily be sustained in the beam chamber. After each bunch passage, when the electrons hit the wall, the density is reduced by several orders of magnitude (see Fig. 7). This suggests that a recurring source of electrons and/or an ingredient that modifies the electron dynamics, e.g. ions, must be present in the chamber.

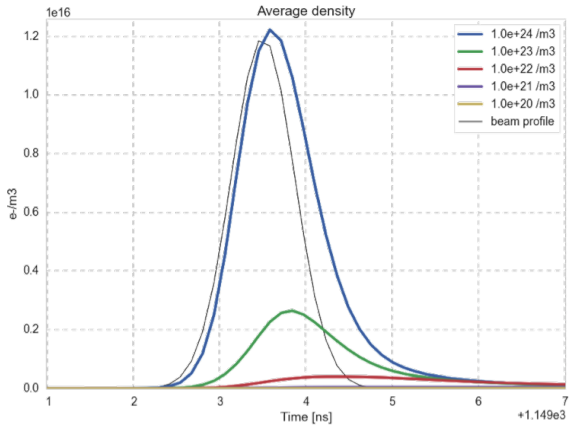

Figure 7: Simulation results of the average electron density during a bunch passage for different N_2 gas densities.

The presence of a high gas density, such as estimated from the loss observations, could generate a high electron density at each bunch passage through beam-induced ionization. Figure 7 shows simulation results of the average electron density during a bunch passage for beam-induced ionization with varying N_2 gas densities. Beam dynamics simulation studies show that beam-induced electrons can induce fast instabilities and tune shifts of 10^{-2} for atomic densities around 10^{26} m^{-3} over 10 cm. However, beam-induced ionization generates electrons and ions in equal amounts. Preliminary simulation studies show that also ions alone can induce fast beam instabilities, if the gas density is above 10^{24} m^{-3}, but the observed tune shifts and intra-bunch motion have not been reproduced. In both cases, the integrated gas densities required to induce fast instabilities in the simulations are larger than the densities estimated from the loss observations.

The simulation studies discussed above consider only the interaction between the beam and one type of particle (electron or ion) at a time, due to the current limitations of the available simulation tools. For typical electron-induced instabilities where the residual pressures are relatively low and the electron population builds up over multiple bunches or trains, while ions are repelled by the beam onto the wall, it can be justified to neglect the presence of ions. However, with the high gas densities expected in 16L2, where high numbers of the two species may be produced over a single bunch passage, the electrons and ions may significantly impact each other's motion. Furthermore, additional gas ionization by the electrons (and potentially ions) moving in the vacuum chamber may also be an important ingredient in the 16L2 events and might enhance the electron and ion densities for a given neutral gas density. Efforts to extend the current simulation tools to model the full beam-electron-ion system as well as the effects of electron-induced ionization are currently on-going [22, 23].

MITIGATION OF DUMP EVENTS

Whereas it proved not to be possible to mitigate the instabilities during dump events, the losses observed in 16L2 were found to be affected by different beam and machine configurations. The current in the dipole corrector MCB.16L2, in the vicinity of the 16L2 quadrupole, was found empirically to have an impact on the losses. A strong correlation was observed between the steady state losses and the corrector current, while the beam orbit was kept fixed by compensating with other corrector magnets [24]. In the range of currents with a beneficial effect on the steady state losses, also the dump events were efficiently mitigated [25]. This allowed a period of 12 days of luminosity production without any premature dumps due to 16L2 events, using the full BCMS beam with 2556 bunches, as foreseen for physics production in 2017. After the subsequent beam screen regeneration, however, the corrector current was no longer sufficient to prevent dump events (see Fig. 2).

Several observations over the run suggested that the losses in 16L2 may be sensitive to electron multipacting. First, during a fill with 50 ns bunch spacing, which is known to significantly suppress electron multipacting with respect to the 25 ns bunch spacing, a reduction was observed in steady state losses per proton [24]. Furthermore, a possible explanation for the beneficial effect of the corrector current on the losses could be provided by the impact of the magnetic field on electron multipacting. Results from electron cloud simulations, Fig. 8a, show that the current of electrons impinging on the chamber walls depends significantly on the magnetic field in the corrector for the standard 25 ns beam [26]. In addition, whereas in a field-free region the full surface is exposed to the electron current, a dipolar magnetic field limits the surface area that is exposed, which may have had an important effect on the losses.

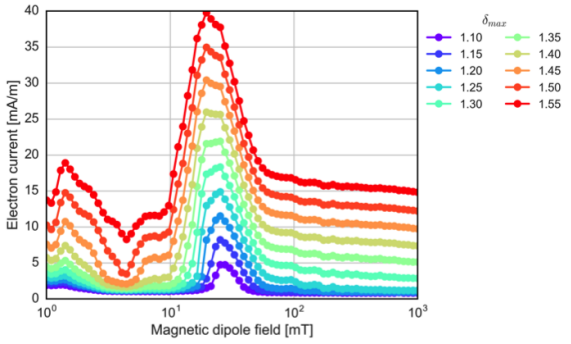

(a) 25 ns beam with 2800 bunches.

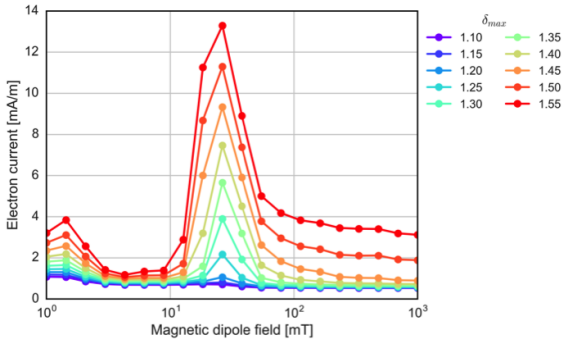

(b) 8b+4e beam with 1900 bunches.

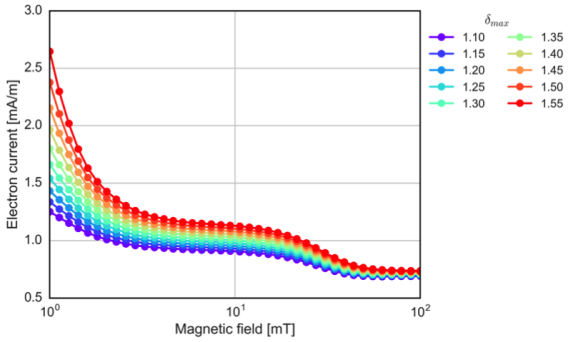

(c) 25 ns beam with 2800 bunches in solenoid field.

Figure 8: Simulation results of the electron current for different beams, magnetic fields and maximum secondary emission yield, $\delta_{\max}$.

A difficult period following the beam screen regeneration, during which attempts to gradually ramp up the bunch intensity and number of bunches to the nominal values failed due to frequent 16L2 events, could be overcome by using an electron-cloud-reducing filling scheme. The 8b+4e bunch pattern, which consists of trains made up of several short trains of eight bunches with 25 ns bunch spacing, separated by four empty slots, was shown in 2015 to effectively suppress electron cloud [27]. The bunch pattern was predicted to significantly reduce the electron current in the sensitive areas in 16L2 compared to the standard 25 ns beam [28], as seen in Figs. 8a and 8b. Operating with the 8b+4e bunch pattern, a significant reduction of UFO-like spikes and dump events was observed, enabling to run stably with nominal bunch intensities of 1.1×10^{11} protons and around 1900 bunches per beam, the maximum number possible for this filling scheme [29].

To further reduce the electron multipacting, a solenoid was installed in the drift space in 16L2 during the second technical stop of the run (TS2) [30]. Simulation results, seen in Fig. 8c, indicate that the solenoid fields achievable with the installed device, around 5 – 10 mT, can reduce the electron current on the chamber walls. Similar solenoid fields were successfully used at CERN in the past to reduce electron cloud in the transfer line between the PS and the SPS [31]. Tests with the solenoid in 16L2 switched variably on and off showed a decrease of steady state losses of 60 – 70% when the solenoid was switched on [32]. With the solenoid, the bunch intensity could be further increased to around 1.25×10^{11} protons for the remainder of the physics run.

IMPACT ON PERFORMANCE

Despite the issue in 16L2, the integrated luminosity delivered to the two main experiments exceeded the target of 45 fb^{-1} set for 2017. This can be attributed in part to the effective mitigation strategies, but also to additional measures implemented in order to increase the instantaneous luminosity. Once stable operation with the 8b+4e beam was established, an alternative production scheme using batch compression (BC), which yields a higher beam brightness, was employed in the injectors to increase the luminosity [33]. In addition, after TS2, the β^* in interaction points 1 and 5 was reduced to 30 cm, further enhancing the instantaneous luminosity [34].

Although the LHC performance was better than predicted in 2017, it was significantly impacted by the 16L2 events. Both the decreased time in physics production due to the premature beam dumps and the limitations on the total beam intensity in order to avoid the events will have degraded the performance. Because the down-time due to 16L2 is visible in the LHC statistics mainly as increased time in operations due to the shortened fill times, rather than as unavailable machine time, its impact on the performance is not straightforward to evaluate [35]. Instead, the 12-day period without 16L2 dumps, enabled by the corrector current mitigation, can be used as a reference period to estimate the luminosity that could have been produced with a similar performance throughout the run.

In practice, the reference period is used to define the average integrated luminosity production per available machine time for the BCMS beam with 2556 bunches. The available time in the absence of 16L2 is then estimated for other parts of the run, by considering the machine to have been available during any down time explicitly caused by 16L2, such as the recovery from a 16L2-induced quench and the time for the beam screen flushing. The projected integrated luminosity based on these considerations is shown in Fig. 9 by the red bars, for different periods as well as over the full run. Any periods that were not strictly dedicated to standard physics production at maximum capacity, such as intensity

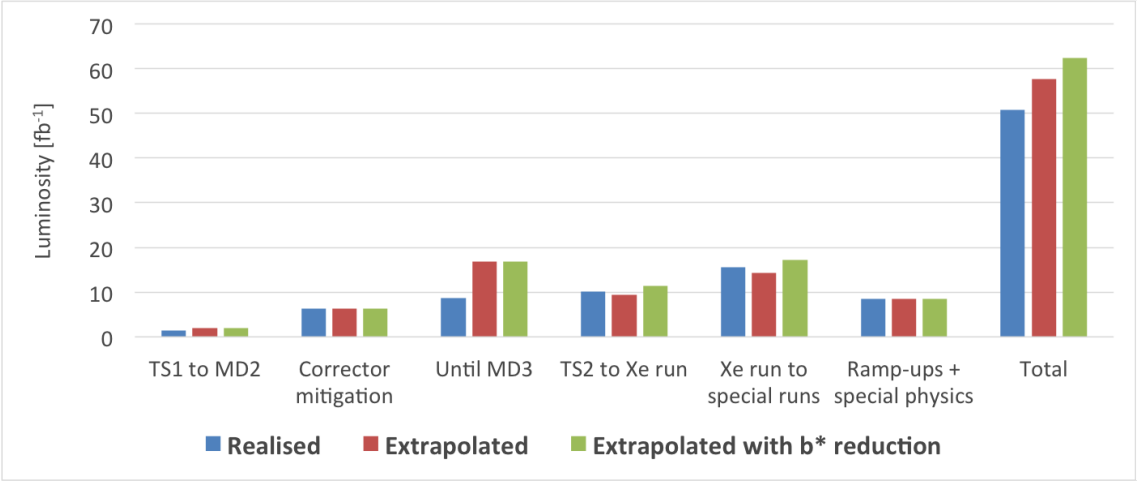

Figure 9: Integrated luminosity in IP 1 and 5 during different periods of the 2017 run. The delivered luminosity (blue) is compared to extrapolated values in the absence of 16L2 events, without (red) and with (green) a reduction in β^* after TS2.

ramp-ups after stops, machine development sessions and special physics runs, have not been included in the analysis and their luminosity is included as such. For comparison, the blue bars in Fig. 9 show the actual delivered luminosity during the run. The largest impact is seen between the corrector current mitigation and the third machine development block (MD3), which was indeed a period with frequent 16L2 events (see Fig. 2). In total, it is estimated that 13% more integrated luminosity could have been produced during the run without the 16L2 events.

After TS2, the delivered integrated luminosity exceeds the projected value, which can be attributed to the increased beam brightness, bunch intensity, and decreased β^* after this period. Luminosity evolution models suggest that similarly increasing the bunch intensity and decreasing the β^* with the full BCMS beam would increase the luminosity compared to the reference case by around 20% [36], yielding a modified projection illustrated by the green bars in Fig. 9. With these additional measures implemented after TS2, it is estimated that the delivered integrated luminosity could have been increased by 23%.

It should be noted that there were additional consequences of the operational scenario that are not considered in this analysis. With the 8b+4e bunch pattern the delivered luminosity was produced with a higher pile-up to luminosity ratio than with the standard beam, which is less favourable for the experiments [37]. In addition, LHCb in particular suffered from the reduced number of bunches and the smaller number of collisions compared to the standard bunch trains.

CONCLUSION

In 2017, the LHC suffered from beam dumps with a characteristic sequence of events that were never observed in the machine before. The problem is now understood to have been caused by the presence of condensed air inside the vacuum chamber, after an accidental air inlet during the cool-down of the affected sector. The observations and analysis summarized in this contribution point to the following explanation for the dump events.

The events were triggered by macro-particles of the frozen air being released and entering the beam. Under certain conditions, the beam could deposit sufficient energy in the macro-particle to induce its phase transition to a gas. This is the key event leading to the runaway conditions that would inevitably lead to a beam dump. The interaction of the beam with the gas resulting from the phase transition could explain both the continued losses and the instabilities associated with 16L2 dumps. More advanced tools that allow detailed modelling of the instability mechanism to support this hypothesis are under development.

Thanks to the realisation that electron cloud played an important role in releasing the macro-particles, stable operation could be restored with measures in place to limit electron cloud production. Together with the steps taken to enhance the luminosity production, excellent LHC performance was achieved. Nevertheless, it is estimated that the integrated luminosity over the year could have been 13-23% higher without the 16L2 events.

ACKNOWLEDGEMENTS

The authors would like to acknowledge the many colleagues who contributed to the understanding of the 16L2 events, in particular in the BE-ABP, BE-BI, BE-OP, BE-RF, EN-STI, TE-CRG, TE-MPE and TE-VSC groups. The authors would also like to thank the LHC Programme Coordination (LPC) and the Availability Working Group (AWG) for the data used in the performance analysis.

REFERENCES

[1] J.M. Jiménez *et al.*, "Observations, analysis and mitigation of recurrent LHC beam dumps caused by fast losses in arc half-cell 16L2", proceedings of IPAC'18, Vancouver, Canada, 2018, paper MOPMF053.

[2] C. Yin Vallgren *et al.*, "16L2 issue: Vacuum observations", presented at LHC Machine Committee (LMC), 16 Aug 2017.

[3] G. Bregliozzi, "ARC12 activities during YETS 2017-2018", presented at LHC Machine Committee (LMC), 20 Dec 2017.

[4] A. Lechner *et al.*, "Update on 16L2 loss observations and BLM threshold changes", presented at LHC Machine Committee (LMC), 16 Aug 2017.

[5] A. Lechner and S. Gilardoni, "Brief update on 16L2 loss observations", presented at LHC Machine Committee (LMC), 16 Aug 2017.

[6] D. Mirarchi and S. Redaelli, "Evolution of losses at 16L2", presented at LHC Machine Committee (LMC), 14 June 2017.

[7] L. Grob *et al.*, "Analysis of loss signatures of unidentified falling objects in the LHC", proceedings of IPAC'18, Vancouver, Canada, 2018, paper TUPAF049.

[8] B. Lindstrom *et al.*, "Results of UFO dynamics studies with beam in the LHC", proceedings of IPAC'18, Vancouver, Canada, 2018, paper THYGBD2.

[9] A. Lechner, "Steady state losses in cell 16L2: loss rate and power deposition studies", presented at LHC Beam Operation Committee (LBOC), 11 Jul 2017.

[10] L. Grob and R. Schmidt, "Input from machine protection / UFO / post mortem analysis", presented at LHC Beam Operation Committee (LBOC), 25 Jul 2017.

[11] A. Lechner *et al.*, "Beam loss measurements for recurring fast loss events during 2017 LHC operation possibly caused by macroparticles", proceedings of IPAC'18, Vancouver, Canada, 2018, paper TUPAF040.

[12] X. Buffat *et al.*, "Observations of coherent motion during dumps on fast losses in IR7", presented at LHC Machine Committee (LMC), 28 June 2017.

[13] X. Buffat *et al.*, "Beam instabilities linked to 16L2", presented at HSC section meeting, 14 Aug 2017.

[14] B. Salvant *et al.*, "Experimental characterisation of a fast instability linked to losses in the 16L2 cryogenic half-cell in the CERN LHC", proceedings of IPAC'18, Vancouver, Canada, 2018, paper THPAF058.

[15] D. Amorim, "Observations of coherent motion during dumps with losses at 16L2", presented at LHC Beam Operation Committee (LBOC), 25 Jul 2017.

[16] L. Mether and G. Rumolo, "Possible mechanism for a fast ion instability in the LHC in the presence of a pressure bump", presented at LHC Beam Operation Committee (LBOC), 11 Jul 2017.

[17] G. Iadarola and G. Rumolo, "Electron Cloud Effects", ICFA Beam Dyn. Newslett. 69 (2016) 208-226.

[18] K. Ohmi, S. Heifets, and F. Zimmermann, "Study of coherent tune shift caused by electron cloud in positron storage rings", proceedings of APAC'01, Beijing, China, 2001.

[19] X. Buffat *et al.*, "Update on observations of coherent motion", presented at 16L2 task force meeting, 5 Sep 2017.

[20] N. Biancacci *et al.*, "Probing the 16L2 instability by an equivalent resonator model", presented at LHC Beam Operation Committee (LBOC), 10 Oct 2017.

[21] E. Métral, "Update on analysis of fast dumps linked to 16L2", presented at LHC Machine Committee (LMC), 12 Jul 2017.

[22] L. Mether, K. Poland, G. Iadarola, and G. Rumolo, "Progress on the understanding of 16L2 events", presented at LHC Beam Operation Committee (LBOC), 31 Jul 2018.

[23] L. Mether, G. Iadarola, K. Poland, and G. Rumolo, "Post e-cloud regime: challenges for multi-species simulations in beam dynamics", proceedings of ECLOUD'18, La Biodola, Italy, 2018.

[24] D. Mirarchi *et al.*, "Update on 16L2 losses", presented at LHC Machine Committee (LMC), 26 Jul 2017.

[25] D. Mirarchi and S. Redaelli, "Evolution of the steady state and fast losses at 16L2", presented at LHC Machine Committee (LMC), 6 Sep 2017.

[26] G. Iadarola *et al.*, "50 ns test and e-cloud considerations", presented at LHC Machine Committee (LMC), 26 Jul 2017.

[27] G. Iadarola *et al.*, "Performance limitations from electron cloud in 2015", proceedings of the 6th Evian Workshop, Evian, 15-17 Dec 2015.

[28] G. Iadarola, L. Bitsikokos, P. Dijkstal, and A. Romano, "E-cloud simulation studies for the 16L2 region", presented at HSC section meeting, 27 Nov 2017.

[29] W. Höfle *et al.*, "LHC status 13th September 2017", presented at LHC Machine Committee (LMC), 13 Sep 2017.

[30] G. Arduini *et al.*, "Resistive solenoid in the 16L2 interconnect", presented at LHC Machine Committee (LMC), 13 Sep 2017.

[31] R. Cappi, M. Giovannozzi, E. Métral, G. Métral, G. Rumolo, and F. Zimmermann, "Electron cloud buildup and related instability in the CERN Proton Synchrotron", Phys. Rev. ST Accel. Beams 5 (2002) 094401.

[32] A. Milanese *et al.*, "Update on solenoid around 16L2", presented at LHC Machine Committee (LMC), 27 Sep 2017.

[33] S. Albright *et al.*, "Overview of the beams from the injectors", these proceedings.

[34] T. Argyropoulos, "LHC Operation: Experience and new tools", these proceedings.

[35] M. Pojer "LHC Operation", these proceedings.

[36] Y. Papaphilippou, private communication, 2017.

[37] J. Boyd and C. Schwick, "Feedback from the experiments on the 2017 run", these proceedings.